

Visual Attention Network

Meng-Hao Guo¹, Cheng-Ze Lu², Zheng-Ning Liu¹,
Ming-Ming Cheng², and Shi-Min Hu¹

¹ BNRist, Department of Computer Science and Technology, Tsinghua University.

² TKLNDST, College of Computer Science, Nankai University.

gmh20@mails.tsinghua.edu.cn, czlu919@outlook.com, lzhengning@gmail.com,
cmm@nankai.edu.cn, shimin@tsinghua.edu.cn

Abstract. While originally designed for natural language processing tasks, the self-attention mechanism has recently taken various computer vision areas by storm. However, the 2D nature of images brings three challenges for applying self-attention in computer vision. (1) Treating images as 1D sequences neglects their 2D structures. (2) The quadratic complexity is too expensive for high-resolution images. (3) It only captures spatial adaptability but ignores channel adaptability. In this paper, we propose a novel large kernel attention (LKA) module to enable self-adaptive and long-range correlations in self-attention while avoiding the above issues. We further introduce a novel neural network based on LKA, namely Visual Attention Network (VAN). While extremely simple, VAN outperforms the state-of-the-art vision transformers and convolutional neural networks with a large margin in extensive experiments, including image classification, object detection, semantic segmentation, instance segmentation, *etc.* Code is available at <https://github.com/Visual-Attention-Network>.

Keywords: Attention, Vision Backbone, Deep Learning, ConvNets

1 Introduction

As the basic feature extractor, vision backbone is a fundamental research topic in the computer vision field. Due to remarkable feature extraction performance, convolutional neural networks (CNNs) [43,42,41] are indispensable topic in the last decade. After the AlexNet [41] reopened the deep learning decade, a number of breakthroughs have been made to get more powerful vision backbones, by using deeper network [70,31], more efficient architecture [33,92,104], stronger multi-scale ability [37,73,21], and attention mechanisms [36,19]. Due to translation invariance property and shared sliding-window strategy [69], CNNs are inherently efficient for various vision tasks with arbitrary sized input. More advanced vision backbone networks often results in significant performance gain in various tasks, including image classification [31,19,54], object detection [16], semantic segmentation [91] and pose estimation [82].

Based on observed reaction times and estimated signal transmission times along biological pathways [23], cognitive psychology [78] and neuroscience [87]

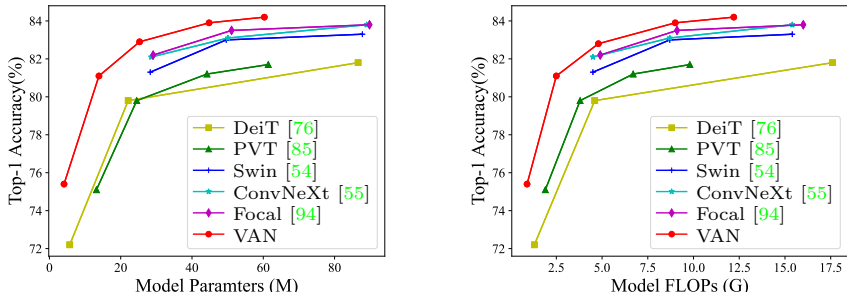


Fig. 1. Results of different models on ImageNet-1K validation set. Left: Comparing the performance of recent models DeiT [76], PVT [85], Swin Transformer [54], ConvNeXt [55], Focal Transformer [94] and our VAN. All these models have a similar amount of parameters. Right: Comparing the performance of recent models and our VAN while keeping the computational cost similar.

researchers believe that human vision system processes only parts of possible stimuli in detail, while leaving the rest nearly unprocessed. Selective attention is an important mechanism for dealing with the combinatorial aspects of complex search in vision [79]. Attention mechanism can be regarded as an adaptive selecting process based on the input feature. Since the fully attention network [80] been proposed, self-attention models (*a.k.a.*, Transformer) quickly becomes the dominated architecture [18,8] in natural language processing (NLP). Recently, Dosovitskiy *et al.* [19] propose the vision transformer (ViT), which introduces transformer backbone into computer vision and outperforms well-known CNNs on image classification tasks. Benefited from its powerful modeling capabilities, transformer-based vision backbones quickly occupy the leaderboards of various tasks, including object detection [54], semantic segmentation [91], *etc.*

Even with remarkable success, convolution operation and self-attention still have their shortcomings. Convolution operation adopts static weight and lacks adaptability, which has been proven critical [36,16]. As originally designed for 1D NLP tasks, self-attention [19,19] regards 2D images as 1D sequences, which destroys the crucial 2D structure of the image. It is also difficult to process high-resolution images due to its quadratic computational and memory overhead. Besides, self-attention is a special attention that only considers the adaptability in spatial dimension but ignores the adaptability in channel dimension, which is also important for visual tasks [36,88,83,1].

In this paper, we propose a novel attention mechanism dubbed large kernel attention (LKA), which is tailored for visual tasks. LKA absorbs the advantages of convolution and self-attention, including local structure information, long-range dependence, and adaptability. Meanwhile, it avoids their disadvantages such as ignoring adaptability in channel dimension. Based on the LKA, we present a novel vision backbone called Visual Attention Network (VAN) that

significantly surpasses well-known CNN-based and transformer-based backbones. The contributions of this paper are summarized as follows:

- We design a novel attention mechanism named LKA for computer vision, which considers the pros of both convolution and self-attention, while avoiding their cons. Based on LKA, we further introduce a simple vision backbone called VAN.
- We show that VANs outperform the state-of-the-art ViTs and CNNs with a large margin in extensive experiments, including image classification, object detection, semantic segmentation, instance segmentation, *etc.*

2 Related Work

2.1 Convolutional Neural Networks

How to effectively compute powerful feature representations is the most fundamental problem in computer vision. The convolutional neural networks (CNNs) [43,42], utilize local contextual information and translation invariance properties to greatly improve the effectiveness of neural networks. CNNs quickly become the mainstream framework in computer vision since AlexNet [41]. To further improve the usability, researchers put lots of effort in making the CNNs deeper [70,31,37,6,73], and lighter [33,67,104]. Our work has similarity with MobileNet [33], which decouples a standard convolution into two parts, a depthwise convolution and a pointwise convolution (*a.k.a.*, 1×1 Conv [45]). Our method decomposes a convolution into three parts: depthwise convolution, depthwise and dilated convolution [12,95], and pointwise convolution. Benefiting from this decomposition, our method is more suitable for efficiently decomposing large kernel convolutions. We also introduce attention mechanism into our method to obtain adaptive property.

2.2 Visual Attention Methods

Attention mechanism can be regarded as an adaptive selection process according to the input feature, which is introduced into computer vision in RAM [58]. It has provided benefits in many visual tasks, such as image classification [36,88], object detection [16,34] and semantic segmentation [98,22]. Attention in computer vision can be divided into four basic categories [27], including channel attention, spatial attention, temporal attention and branch attention, and their combinations such as channel & spatial attention. Each kind of attention has a different effect in visual tasks.

Originating from NLP [80,18], self-attention is a special kind of attention mechanism. Due to its effectiveness of capturing the long-range dependence and adaptability, it is playing an increasingly important role in computer vision [86,20,64,7,99,101,93]. Various deep self-attention networks (*a.k.a.*, vision transformers) [19,10,54,24,71,85,97,49,5,50,4,52,89,53,29] have achieved significantly

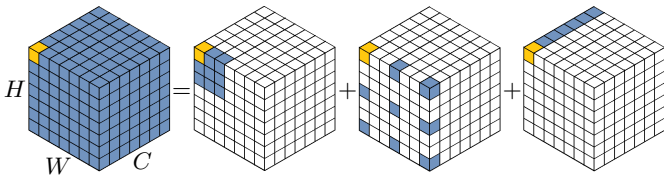


Fig. 2. Decomposition diagram of large-kernel convolution. A standard convolution can be decomposed into three parts: a depth-wise convolution (DW-Conv), a depth-wise dilation convolution (DW-D-Conv), and a pointwise convolution (1×1 Conv). The colored grids represent the location of convolution kernel and the yellow grid means the center point. The diagram shows that a 13×13 convolution is decomposed into a 5×5 depth-wise convolution, a 5×5 depth-wise dilation convolution with dilation rate 3, and a pointwise convolution. Note: zero paddings are omitted in the above figure.

better performance than the mainstream CNNs on different visual tasks, showing the huge potential of attention-based models. However, self-attention is originally designed for NLP. It has three shortcomings when dealing with computer vision tasks. (1) It treats images as 1D sequences which neglects the 2D structure of images. (2) The quadratic complexity is too expensive for high-resolution images. (3) It only achieves spatial adaptability but ignores the adaptability in channel dimension. For vision tasks, different channels often represent different objects [13,27]. Channel adaptability is also proven important for visual tasks [36,88,62,83,13]. To solve these problems, we propose a novel visual attention method, namely, LKA. It involves the pros of self-attention such as adaptability and long-range dependence. Besides, it benefits from the advantages of convolution such as making use of local contextual information.

2.3 Vision MLPs

Multilayer Perceptrons (MLPs) [65,66] were a popular tool for computer vision before CNNs appearing. However, due to high computational requirements and low efficiency, the capability of MLPs was been limited in a long time. Some recent research successfully decouple standard MLP into spatial MLP and channel MLP [74,25,75,48]. Such decomposition allows significant computational cost and parameters reduction, which release the amazing performance of MLP. Readers are referred to recent surveys [26,51] for a more comprehensive review of MLPs. The most related MLP to our method is the gMLP [48], which not only decomposes the standard MLP but also involves the attention mechanism. However, gMLP has two drawbacks. On the one hand, gMLP is sensitive to input size and can only process fixed-size images. On the other hand, gMLP only considers the global information of the image and ignore their local structure. Our method can make full use of its advantages and avoid its shortcomings.

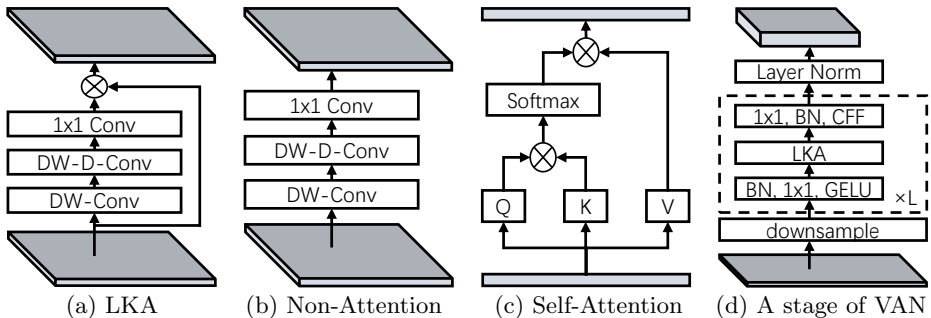


Fig. 3. The structure of different modules: (a) the proposed Large Kernel Attention (LKA); (b) non-attention module; (c) the self-attention module [80]; (d) a stage of our Visual Attention Network (VAN). CFF means convolutional feed-forward network. Residual connection [31] is omitted in (d). The difference between (a) and (b) is the element-wise multiply. It is worth noting that (c) is designed for 1D sequences.

3 Method

3.1 Large Kernel Attention

Attention mechanism can be regarded as an adaptive selection process, which can select the discriminative features and automatically ignore noisy responses according to the input features. The key step of attention mechanism is producing attention map which indicates the importance of different parts. To do so, we should learn the relationship between them.

There are two well-known methods to build relationship between different parts. The first one is adopting self-attention mechanism [86,99,101,19] to capture long-range dependence. There are three obvious shortcomings for self-attention applied in computer vision which have been listed in Sec. 2.2. The second one is to use large kernel convolution [88,81,35,60] to build relevance and produce attention map. There are still obvious cons in this way. Large-kernel convolution brings a huge amount of computational overhead and parameters.

To overcome above listed cons and make use of the pros of self-attention and large kernel convolution, we propose to decompose a large kernel convolution operation to capture long-range relationship. As shown in Fig. 2, a large kernel convolution can be divided into three components: a spatial local convolution (depth-wise convolution), a spatial long-range convolution (depth-wise dilation convolution), and a channel convolution (1×1 convolution). Specifically, a $K \times K$ convolution is decomposed into a $\lceil \frac{K}{d} \rceil \times \lceil \frac{K}{d} \rceil$ depth-wise dilation convolution with dilation d , a $(2d - 1) \times (2d - 1)$ depth-wise convolution and a 1×1 convolution. Through the above decomposition, the module can capture long-range relationship with slight computational cost and parameters. After obtaining long-range relationship, we can estimate the importance of a point and generate attention

Table 1. Desirable properties belonging to convolution, self-attention and LKA.

Properties	Convolution	Self-Attention	LKA
Local Receptive Field	✓	✗	✓
Long-range Dependence	✗	✓	✓
Spatial Adaptability	✗	✓	✓
Channel Adaptability	✗	✗	✓

map. As demonstrated in Fig. 3(a), the LKA module can be written as

$$Attention = Conv_{1 \times 1}(DW-D-Conv(DW-Conv(F))), \quad (1)$$

$$Output = Attention \otimes F. \quad (2)$$

Here, $F \in \mathbb{R}^{C \times H \times W}$ is the input feature. $Attention \in \mathbb{R}^{C \times H \times W}$ denotes attention map. The value in attention map indicates the importance of each feature. \otimes means element-wise product. As shown in Tab. 1, our proposed LKA combines the advantages of convolution and self-attention. It takes the local contextual information, large receptive field, and dynamic process into consideration. Furthermore, LKA not only achieves the adaptability in the spatial dimension but also the adaptability in the channel dimension. It worth noting that different channels often represent different objects in deep neural networks [27,13] and adaptability in the channel dimension is also important for visual tasks.

3.2 Visual Attention Network (VAN)

Our VAN has a simple hierarchical structure, *i.e.*, a sequence of four stages with decreasing output spatial resolution, *i.e.*, $\frac{H}{4} \times \frac{W}{4} \times C$, $\frac{H}{8} \times \frac{W}{8} \times C$, $\frac{H}{16} \times \frac{W}{16} \times C$ and $\frac{H}{32} \times \frac{W}{32} \times C$ respectively. Here, H and W donate the height and width of the input image. With the decreasing of resolution, the number of output channels is increasing. The change of output channel C_i is presented in Tab. 2.

For each stage as shown in Fig. 3 (d), we firstly downsample the input and use the stride number to control the downsample rate. After the downsample,

Table 2. The detailed setting for different versions of the VAN. e.r. represents expansion ratio in the feed-forward network.

stage	output size	e.r.	VAN-Tiny	VAN-Small	VAN-Base	VAN-Large	VAN-Huge
1	$\frac{H}{4} \times \frac{W}{4} \times C$	8	$C = 32$ $L = 3$	$C = 64$ $L = 2$	$C = 64$ $L = 3$	$C = 64$ $L = 3$	$C = 64$ $L = 3$
2	$\frac{H}{8} \times \frac{W}{8} \times C$	8	$C = 64$ $L = 3$	$C = 128$ $L = 2$	$C = 128$ $L = 3$	$C = 128$ $L = 5$	$C = 128$ $L = 6$
3	$\frac{H}{16} \times \frac{W}{16} \times C$	4	$C = 160$ $L = 5$	$C = 320$ $L = 4$	$C = 320$ $L = 12$	$C = 320$ $L = 27$	$C = 320$ $L = 40$
4	$\frac{H}{32} \times \frac{W}{32} \times C$	4	$C = 256$ $L = 2$	$C = 512$ $L = 2$	$C = 512$ $L = 3$	$C = 512$ $L = 3$	$C = 512$ $L = 3$
Parameters (M)			4.1	13.9	26.6	44.8	60.3
FLOPs (G)			0.9	2.5	5.0	9.0	12.2

Table 3. Number of parameters for different forms of a 21×21 convolution. For instance, when the number of channels $C = 32$, standard convolution and MobileNet decomposition use $133\times$ and $4.5\times$ more parameters than our decomposition respectively.

	Standard Convolution	Decomposition Type	
		MobileNet [33]	Ours
C=32	451,584	15,136	3,392
C=64	1,806,336	32,320	8,832
C=128	7,225,344	72,832	25,856
C=256	28,901,376	178,432	84,480
C=512	115,605,504	487,936	300,032

Table 4. Ablation study of different modules in LKA. Top-1 accuracy (Acc) on ImageNet validation set suggest that each part is critical. w/o Attention means we adopt Fig. 3(b).

VAN-Tiny	Acc(%)
w/o DW-Conv	74.9
w/o DW-D-Conv	74.1
w/o Attention	74.3
w/o 1×1 Conv	74.6
All	75.4

all other layers in a stage stay the same output size, *i.e.*, spatial resolution and the number of channels. Then, L groups of batch normalization [38], 1×1 Conv, GELU activation [32], large kernel attention and convolutional feed-forward network (CFF) [84] are stacked in sequence to extract features. Finally, we apply a layer normalization [2] at the end of each stage. We design five architectures VAN-Tiny, VAN-Small, VAN-Base, VAN-Large and VAN-Huge according to the parameters and computational cost. The details of the whole network are shown in Tab. 2.

Complexity analysis. We present the parameters and floating point operations (FLOPs) of our decomposition. Bias is omitted in the computation process for simplifying format. We assume that the input and output features have same size $H \times W \times C$. The parameters and FLOPs can be donated as:

$$\mathbf{Params} = \lceil \frac{K}{d} \rceil \times \lceil \frac{K}{d} \rceil \times C + (2d - 1) \times (2d - 1) \times C + C \times C, \quad (3)$$

$$\mathbf{FLOPs} = (\lceil \frac{K}{d} \rceil \times \lceil \frac{K}{d} \rceil \times C + (2d - 1) \times (2d - 1) \times C + C \times C) \times H \times W. \quad (4)$$

Here, d means dilation rate and K is kernel size. According to the formula of FLOPs and parameters, the ratio of budget saving is the same for FLOPs and parameters.

Implementation details. When $K = 21$, the Equ. (3) can be written as:

$$\mathbf{Params} = (\lceil \frac{21}{d} \rceil \times \lceil \frac{21}{d} \rceil + (2d - 1) \times (2d - 1)) \times C + C \times C, d \in Z^+. \quad (5)$$

We find that when $d = 3$, the Equ. (5) takes the minimum value. So, we set $d = 3$ by default when $K = 21$, which corresponds to 5×5 depth-wise convolution and 7×7 depth-wise convolution with dilation 3. For different number of channels, we show the specific parameters in Tab. 3. It shows that our decomposition owns significant advantages in decomposing large kernel convolution in terms of parameters and FLOPs.

Table 5. Ablation study of different kernel size in LKA. Acc(%) means Top-1 accuracy on ImageNet validation set.

Method	Kernel size	Dilation	Params. (M)	GFLOPs	Acc(%)
VAN-Tiny	7	2	4.03	0.85	74.8
VAN-Tiny	14	3	4.07	0.87	75.3
VAN-Tiny	21	3	4.11	0.88	75.4
VAN-Tiny	28	4	4.14	0.90	75.4
VAN-Tiny	35	4	4.20	0.92	75.6

4 Experiments

In this section, quantitative and qualitative experiments are exhibit to demonstrate the effectiveness of the proposed VAN. We conduct quantitative experiments on ImageNet-1K [17] image classification dataset, COCO [47] object detection dataset and ADE20K [107] semantic segmentation dataset. Furthermore, we visualize the class activation mapping(CAM) [106] by using Grad-CAM [68] on ImageNet validation set. All models are trained with 8 RTX 3090 or A100 GPUs.

4.1 Image Classification

Settings. We conduct image classification on ImageNet-1K [17] dataset. It contains 1.28M training images and 50K validation images from 1,000 different categories. The whole training scheme mostly follows [76]. We adopt random clipping, random horizontal flipping, label-smoothing [59], mixup [102], cutmix [100] and random erasing [105] to augment the training data. In the training process, we train our VAN for 310 epochs by using AdamW [39,57] optimizer with momentum=0.9, weight decay= 5×10^{-2} and batch size = 1,024. Cosine schedule [56] and warm-up strategy are employed to adjust the learning rate(LR). The initial LR is set to 5×10^{-4} . We adopt a variant of LayerScale [77] in attention layer which replaces $x_{out} = x + diag(\lambda_1, \lambda_2, \dots, \lambda_d)f(x)$ with $x_{out} = x + diag(\lambda_1, \lambda_2, \dots, \lambda_d)(f(x) + x)$ with initial value 0.01 and achieves a better performance than original LayerScale. Exponential moving average (EMA) [61] is also applied to improve training process. During the eval stage, we report the top-1 accuracy on ImageNet validation set under single crop setting.

Ablation Study. We conduct an ablation study to prove that each component of LKA is critical. In order to obtain experimental results quickly, we choose VAN-Tiny as our baseline model. The experimental results in the Tab. 4 indicate that all components in LKA are indispensable to improve performance.

- **DW-Conv.** DW-Conv can make use of the local contextual information of images. Without it, the classification performance will drop by 0.5% (74.9% vs. 75.4%), showing the importance of local structural information in image processing.

Table 6. Compare with the state-of-the-art methods on ImageNet validation set. Params means parameter. GFLOPs donates floating point operations. Top-1 Acc represents Top-1 accuracy.

Method	Params. (M)	GFLOPs	Top-1 Acc (%)
PVTv2-B0 [84]	3.4	0.6	70.5
T2T-ViT-7 [97]	4.3	1.1	71.7
DeiT-Tiny/16 [76]	5.7	1.3	72.2
TNT-Ti [28]	6.1	1.4	73.9
VAN-Tiny	4.1	0.9	75.4
ResNet18 [31]	11.7	1.8	69.8
PVT-Tiny [85]	13.2	1.9	75.1
PoolFormer-S12 [96]	11.9	2.0	77.2
PVTv2-B1 [84]	13.1	2.1	78.7
VAN-Small	13.9	2.5	81.1
ResNet50 [31]	25.6	4.1	76.5
ResNeXt50-32x4d [92]	25.0	4.3	77.6
RegNetY-4G [63]	21.0	4.0	80.0
DeiT-Small/16 [76]	22.1	4.6	79.8
T2T-ViT _t -14 [97]	21.5	6.1	81.7
PVT-Small [85]	24.5	3.8	79.8
TNT-S [28]	23.8	5.2	81.3
ResMLP-24 [75]	30.0	6.0	79.4
gMLP-S [48]	20.0	4.5	79.6
Swin-T [54]	28.3	4.5	81.3
PoolFormer-S24 [96]	21.4	3.6	80.3
Twins-SVT-S [14]	24.0	2.8	81.7
PVTv2-B2 [84]	25.4	4.0	82.0
Focal-T [94]	29.1	4.9	82.2
ConvNeXt-T [55]	28.6	4.5	82.1
VAN-Base	26.6	5.0	82.8
ResNet101 [31]	44.7	7.9	77.4
ResNeXt101-32x4d [92]	44.2	8.0	78.8
Mixer-B/16 [74]	59.0	11.6	76.4
T2T-ViT _t -19 [97]	39.2	9.8	82.4
PVT-Medium [85]	44.2	6.7	81.2
Swin-S [54]	49.6	8.7	83.0
ConvNeXt-S [54]	50.1	8.7	83.1
PVTv2-B3 [84]	45.2	6.9	83.2
Focal-S [94]	51.1	9.1	83.5
VAN-Large	44.8	9.0	83.9
ResNet152 [31]	60.2	11.6	78.3
T2T-ViT _t -24 [97]	64.0	15.0	82.3
PVT-Large [85]	61.4	9.8	81.7
TNT-B [28]	66.0	14.1	82.8
PVTv2-B4 [84]	62.6	10.1	83.6
VAN-Huge	60.3	12.2	84.2

- **DW-D-Conv.** DW-D-Conv donates depth-wise dilation convolution which plays a role in capturing long-range dependence in LKA. Without it, the classification performance will drop by 1.3% (74.1% vs. 75.4%) which confirms our viewpoint of long-range dependence is critical for visual tasks.

- **Attention Mechanism.** The introduction of the attention mechanism can be regarded as making network achieve adaptive property. Benefited from it, the VAN-Tiny achieves about 1.1% (74.3% vs. 75.4%) improvement.
- 1×1 **Conv.** Here, 1×1 Conv captures relationship in channel dimension. Combining with attention mechanism, it introduces adaptability in channel dimension. It brings about 0.8% (74.6% vs. 75.4%) improvement which proves the necessity of the adaptability in channel dimension.

Through the above analysis, we can find that our proposed LKA can utilize local information, capture long-distance dependencies, and have adaptability in both channel and spatial dimension. Furthermore, experimental results prove all properties are positive for recognition tasks. Although standard convolution can make full use of the local contextual information, it ignores long-range dependencies and adaptability. As for self-attention, although it can capture long-range dependencies and has adaptability in spatial dimensions, it neglects the local information and the adaptability in the channel dimension. Meanwhile, We also summarize above discussion in Tab. 1.

Besides, we also conduct ablation study to decompose different size convolution kernels in Tab. 5. We can find that decomposing a 21×21 convolution works better than decomposing a 7×7 convolution which demonstrates large kernel is critical for visual tasks. Decomposing a larger 35×35 convolution, we find the gain is not obvious comparing with decomposing a 21×21 convolution. Thus, we choose to decompose a 21×21 convolution by default.

Comparison with Existing Methods. Tab. 6 presents the comparison of VAN with other MLPs, CNNs and ViTs. VAN outperforms common CNNs (ResNet [31], ResNeXt [92], ConvNeXt [55], *etc.*), ViTs (DeiT [76], PVT [85] and Swin-Transformer [54], *etc.*) and MLPs (MLP-Mixer [74], ResMLP [75], gMLP [48], *etc.*) with similar parameters and computational cost. In the following discussion, we will choose a representative network in each category.

ConvNeXt [55] is a special CNN which absorbs the some advantages of ViTs such as large receptive field (7×7 convolution) and advanced training strategy(300 epochs, data augmentation, *etc.*). Compared VAN with ConvNeXt [55], VAN-Base surpasses ConvNeXt-T by 0.7% (82.8% vs. 82.1%) since VAN has larger receptive field and adaptive ability. Swin-Transformer is a well-known ViT variant that adopts local attention and shifted window manner. Due to that VAN is friendly for 2D structural information, has larger receptive field and achieves adaptability in channel dimension, VAN-Base surpasses Swin-T by 1.5% (82.8% vs. 81.3%). As for MLPs, we choose gMLP [48]. VAN-Base surpass gMLP-S [48] by 3.2% (82.8% vs. 79.6%) which reflects the importance of locality.

Visualization Class activation mapping (CAM) is a popular tool to visualize the discriminative regions (attention maps). We adopt Grad-CAM [68] to visualize the attentions on the ImageNet validation set produced by VAN-Base model. Results in Fig. 4 show that VAN-Base can clearly focus on the target objects. Thus, the visualizations intuitively demonstrate the effectiveness of our

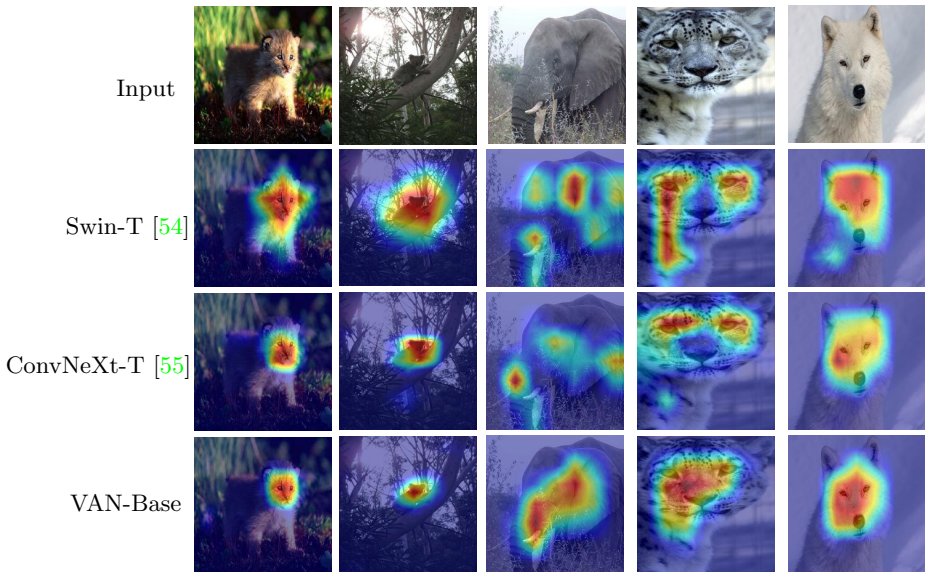


Fig. 4. Visualization results. All images come from different categories in ImageNet validation set. CAM is produced by using Grad-CAM [68]. We compare different CAMs produced by Swin-T [54], ConvNeXt-T [55] and VAN-Base.

method. Furthermore, we also compare different CAM produced by Swin-T [54], ConvNeXt-T [55] and VAN-Base. We can find that the activation area of VAN-Base is more accurate. In particular, our method shows obvious advantages when the object is dominant in an image, which demonstrates its ability to capture long-range dependence.

4.2 Object Detection

Settings. We conduct object detection and instance segmentation experiments on COCO 2017 benchmark [47], which contains 118K images in training set and 5K images in validation set. MMDetection [11] is used as the codebase to implement detection models. For fair comparison, we adopt the same training/validating strategies with Swin Transformer [54] and PoolFormer [96]. Many kinds of detection models (*e.g.*, Mask R-CNN [30], RetinaNet [46], Cascade Mask R-CNN [9], Sparse R-CNN [72], *etc.*) are included to demonstrate the effectiveness of our method. All backbone models are pre-trained on ImageNet training set.

Results. According to Tab. 7 and Tab. 8, we find that VAN surpasses CNN-based method ResNet [31] and transformer-based method PVT [85] with a large margin under RetinaNet [46] 1x and Mask R-CNN [30] 1x settings. Besides, we also compare the state-of-the-art methods Swin transformer [54] and ConvNeXt [55] in Tab. 9. Results show that VAN achieves the state-of-the-art

Table 7. Object detection on COCO 2017 dataset. #P means parameter. RetinaNet 1× donates models are based on RetinaNet [46] and we train them for 12 epochs.

Backbone	RetinaNet 1×						
	#P (M)	AP	AP ₅₀	AP ₇₅	AP _S	AP _M	AP _L
VAN-Tiny	13.4	38.8	58.8	41.3	23.4	42.8	50.9
ResNet18 [31]	21.3	31.8	49.6	33.6	16.3	34.3	43.2
PoolFormer-S12 [85]	21.7	36.2	56.2	38.2	20.8	39.1	48.0
PVT-Tiny [85]	23.0	36.7	56.9	38.9	22.6	38.8	50.0
VAN-Small	23.6	42.3	63.1	45.1	26.1	46.2	54.1
ResNet50 [31]	37.7	36.3	55.3	38.6	19.3	40.0	48.8
PVT-Small [85]	34.2	40.4	61.3	43.0	25.0	42.9	55.7
PoolFormer-S24 [96]	31.1	38.9	59.7	41.3	23.3	42.1	51.8
PoolFormer-S36 [96]	40.6	39.5	60.5	41.8	22.5	42.9	52.4
VAN-Base	36.3	44.9	65.7	48.4	27.4	49.2	58.7
ResNet101 [31]	56.7	38.5	57.8	41.2	21.4	42.6	51.1
PVT-Medium [85]	53.9	41.9	63.1	44.3	25.0	44.9	57.6
VAN-Large	54.5	46.1	67.0	49.7	28.4	50.1	59.8

Table 8. Object detection and instance segmentation on COCO 2017 dataset. #P means parameter. Mask R-CNN 1× donates models are based on Mask R-CNN [30] and we train them for 12 epochs. AP^b and AP^m refer to bounding box AP and mask AP respectively.

Backbone	Mask R-CNN 1×						
	#P (M)	AP ^b	AP ₅₀ ^b	AP ₇₅ ^b	AP ^m	AP ₅₀ ^m	AP ₇₅ ^m
VAN-Tiny	23.9	40.2	62.6	44.4	37.6	59.6	40.4
ResNet18 [31]	31.2	34.0	54.0	36.7	31.2	51.0	32.7
PoolFormer-S12 [96]	31.6	37.3	59.0	40.1	34.6	55.8	36.9
PVT-Tiny [85]	32.9	36.7	59.2	39.3	35.1	56.7	37.3
VAN-Small	33.5	42.6	64.2	46.7	38.9	61.2	41.7
ResNet50 [31]	44.2	38.0	58.6	41.4	34.4	55.1	36.7
PVT-Small [85]	44.1	40.4	62.9	43.8	37.8	60.1	40.3
PoolFormer-S24 [96]	41.0	40.1	62.2	43.4	37.0	59.1	39.6
PoolFormer-S36 [96]	50.5	41.0	63.1	44.8	37.7	60.1	40.0
VAN-Base	46.2	46.4	67.8	51.0	41.8	65.2	44.9
ResNet101 [31]	63.2	40.4	61.1	44.2	36.4	57.7	38.8
ResNeXt101-32x4d [92]	62.8	41.9	62.5	45.9	37.5	59.4	40.2
PVT-Medium [85]	63.9	42.0	64.4	45.6	39.0	61.6	42.1
VAN-Large	64.4	47.1	67.9	51.9	42.2	65.4	45.5

performance with different detection methods such as Mask R-CNN [30] and Sparse R-CNN [72].

4.3 Semantic Segmentation

Settings. We conduct experiments on ADE20K [107], which contains 150 semantic categories for semantic segmentation. It consists of 20,000, 2,000 and

Table 9. Comparison with the state-of-the-art vision backbones on COCO 2017 benchmark. All models are trained for 36 epochs. We calculate FLOPs with input size of $1,280 \times 800$.

Backbone	Method	AP ^b	AP ^b ₅₀	AP ^b ₇₅	#P (M)	GFLOPs
Swin-T [31]		46.0	68.1	50.3	48	264
ConvNeXt-T [54]	Mask R-CNN [30]	46.2	67.9	50.8	48	262
VAN-Base		47.4	68.6	51.6	46	273
ResNet50 [31]		46.3	64.3	50.5	82	739
Swin-T [54]	Cascade	50.5	69.3	54.9	86	745
ConvNeXt-T [55]	Mask R-CNN [9]	50.4	69.1	54.8	86	741
VAN-Base		50.5	69.3	54.6	84	752
ResNet50 [31]		43.5	61.9	47.0	32	205
Swin-T [54]	ATSS [103]	47.2	66.5	51.3	36	215
VAN-Base		49.1	68.2	53.3	34	221
ResNet50 [31]		44.5	63.0	48.3	32	208
Swin-T [54]	GFL [44]	47.6	66.8	51.7	36	215
VAN-Base		49.3	68.5	53.5	34	224
ResNet50 [31]		44.5	63.4	48.2	106	166
Swin-T [54]	Sparse R-CNN [72]	47.9	67.3	52.3	110	172
VAN-Base		49.1	68.9	53.6	108	178

3,000 separately for training, validation and testing. MMSEG [15] is used as the base framework and two famous segmentation heads, Semantic FPN [40] and UperNet [90], are employed for evaluating our VAN backbones. For a fair comparison, we adopt two training/validating schemes following [96] and [54] and quantitative results on the validation set are shown in the upper and lower part in Tab. 10, respectively. All backbone models are pre-trained on ImageNet training set.

Results. From the upper part in Tab. 10, compared with different backbones using FPN [40], VAN-based methods are superior to CNN-based (ResNet [31], ResNeXt [92]) or transformer-based (PVT [85], PoolFormer [96], PVTv2 [84]) methods. For instance, we surpass four PVTv2 [84] variants by +1.3 (tiny), +0.4 (small), +1.5 (base), +0.8 (large) mIoU under comparable parameters and FLOPs. In the lower part in Tab. 10, when compared with previous state-of-the-art CNN-based methods and Swin-Transformer based methods, four VAN variants also show excellent performance with comparable parameters and FLOPs. For instance, based on UperNet [90], VAN-Base is +3.4 and +2.2 mIoU higher than ResNet-101 and Swin-T, respectively.

5 Future Work

In the future, we will continue perfecting VAN in followings directions:

- **Continuous improvement of the structure itself.** In this paper, we only demonstrate an intuitive structure. There are a lot of potential improvements

Table 10. Results of semantic segmentation on ADE20K [107] validation set. The upper and lower part are obtained under two different training/validation schemes following [96] and [54]. We calculate FLOPs with input size 512×512 for Semantic FPN [40] and $2,048 \times 512$ for UperNet [90].

Method	Backbone	#Param (M)	GFLOPs	mIoU (%)
Semantic FPN [40]	PVTv2-B0 [84]	8	25	37.2
	VAN-Tiny	8	26	38.5
	ResNet18 [31]	16	32	32.9
	PVT-Tiny [85]	17	33	35.7
	PoolFormer-S12 [96]	16	31	37.2
	PVTv2-B1 [84]	18	34	42.5
	VAN-Small	18	35	42.9
	ResNet50 [31]	29	46	36.7
	PVT-Small [85]	28	45	39.8
	PoolFormer-S24 [96]	23	39	40.3
	PVTv2-B2 [84]	29	46	45.2
	VAN-Base	30	48	46.7
	ResNet101 [31]	48	65	38.8
	ResNeXt101-32x4d [92]	47	65	39.7
	PVT-Medium [85]	48	61	43.5
	PoolFormer-S36 [96]	35	48	42.0
PVTv2-B3 [84]	49	62	47.3	
VAN-Large	49	68	48.1	
UperNet [90]	ResNet-101 [31]	86	1029	44.9
OCRNet [98]		56	923	45.3
HamNet [22]		69	1111	46.8
UperNet [90]	Swin-T [54]	60	945	46.1
	Swin-S [54]	81	1038	49.3
	VAN-Tiny	32	858	41.1
	VAN-Small	44	895	44.9
	VAN-Base	57	948	48.3
	VAN-Large	75	1030	50.1

such as adopting different kernel size, introducing multi-scale structure [21] and using multi-branch structure [73].

- **Large-scale self-supervised learning and transfer learning.** VAN naturally combines the advantages of CNNs and ViTs. On the one hand, VAN can make use of the 2D structure information of images. On the other hand, VAN can dynamically adjust the output according to the input image which is suit for self-supervised learning and transfer learning [4,29]. Combining the above two points, we believe VAN can achieve better performance in image self-supervised learning and transfer learning field.
- **More application areas.** Due to the limited resource, we only show excellent performance in visual tasks. Whether VANs can perform well in other

areas like TCN [3] in NLP is still worth exploring. we look forward to seeing VANs becoming a general model.

6 Conclusion

In this paper, we present a novel visual attention LKA which combines the advantages of convolution and self-attention. Based on LKA, we build a vision backbone VAN that achieves the state-of-the-art performance in some visual tasks, including image classification, object detection, semantic segmentation, *etc.* In the future, we will continue to improve this framework from the directions mentioned in Sec. 5.

7 Acknowledgement

This work was supported by the National Key R&D Program(), the Natural Science Foundation of China (Project 61521002, 61922046), and Tsinghua-Tencent Joint Laboratory for Internet Innovation Technology.

References

1. Ali, A., Touvron, H., Caron, M., Bojanowski, P., Douze, M., Joulin, A., Laptev, I., Neverova, N., Synnaeve, G., Verbeek, J., et al.: Xcit: Cross-covariance image transformers. *Adv. Neural Inform. Process. Syst.* **34** (2021)
2. Ba, J.L., Kiros, J.R., Hinton, G.E.: Layer normalization (2016)
3. Bai, S., Kolter, J.Z., Koltun, V.: An empirical evaluation of generic convolutional and recurrent networks for sequence modeling. *arXiv preprint arXiv:1803.01271* (2018)
4. Bao, H., Dong, L., Piao, S., Wei, F.: BEit: BERT pre-training of image transformers. In: *Int. Conf. Learn. Represent.* (2022)
5. Bello, I.: Lambdanetworks: Modeling long-range interactions without attention. In: *International Conference on Learning Representations* (2021)
6. Bello, I., Fedus, W., Du, X., Cubuk, E.D., Srinivas, A., Lin, T.Y., Shlens, J., Zoph, B.: Revisiting resnets: Improved training and scaling strategies. *Advances in Neural Information Processing Systems* **34** (2021)
7. Bello, I., Zoph, B., Vaswani, A., Shlens, J., Le, Q.V.: Attention augmented convolutional networks. In: *Proceedings of the IEEE/CVF International Conference on Computer Vision (ICCV)* (October 2019)
8. Brown, T., Mann, B., Ryder, N., Subbiah, M., Kaplan, J.D., Dhariwal, P., Neelakantan, A., Shyam, P., Sastry, G., Askell, A., et al.: Language models are few-shot learners. *Adv. Neural Inform. Process. Syst.* **33**, 1877–1901 (2020)
9. Cai, Z., Vasconcelos, N.: Cascade r-cnn: High quality object detection and instance segmentation. *IEEE Transactions on Pattern Analysis and Machine Intelligence* (2019)
10. Carion, N., Massa, F., Synnaeve, G., Usunier, N., Kirillov, A., Zagoruyko, S.: End-to-end object detection with transformers. In: *Eur. Conf. Comput. Vis.* pp. 213–229. Springer (2020)
11. Chen, K., Wang, J., Pang, J., Cao, Y., Xiong, Y., Li, X., Sun, S., Feng, W., Liu, Z., Xu, J., et al.: Mmdetection: Open mmlab detection toolbox and benchmark. *arXiv preprint arXiv:1906.07155* (2019)
12. Chen, L.C., Papandreou, G., Kokkinos, I., Murphy, K., Yuille, A.L.: Semantic image segmentation with deep convolutional nets and fully connected crfs. *arXiv preprint arXiv:1412.7062* (2014)
13. Chen, L., Zhang, H., Xiao, J., Nie, L., Shao, J., Liu, W., Chua, T.S.: Sca-cnn: Spatial and channel-wise attention in convolutional networks for image captioning. In: *IEEE Conf. Comput. Vis. Pattern Recog.* pp. 5659–5667 (2017)
14. Chu, X., Tian, Z., Wang, Y., Zhang, B., Ren, H., Wei, X., Xia, H., Shen, C.: Twins: Revisiting the design of spatial attention in vision transformers. *Adv. Neural Inform. Process. Syst.* **34** (2021)
15. Contributors, M.: MMSegmentation: Openmmlab semantic segmentation toolbox and benchmark. <https://github.com/open-mmlab/mms Segmentation> (2020)
16. Dai, J., Qi, H., Xiong, Y., Li, Y., Zhang, G., Hu, H., Wei, Y.: Deformable convolutional networks. In: *Int. Conf. Comput. Vis.* pp. 764–773 (2017)
17. Deng, J., Dong, W., Socher, R., Li, L.J., Li, K., Fei-Fei, L.: Imagenet: A large-scale hierarchical image database. In: *2009 IEEE conference on computer vision and pattern recognition.* pp. 248–255. Ieee (2009)
18. Devlin, J., Chang, M.W., Lee, K., Toutanova, K.: Bert: Pre-training of deep bidirectional transformers for language understanding. *arXiv preprint arXiv:1810.04805* (2018)

19. Dosovitskiy, A., Beyer, L., Kolesnikov, A., Weissenborn, D., Zhai, X., Unterthiner, T., Dehghani, M., Minderer, M., Heigold, G., Gelly, S., et al.: An image is worth 16x16 words: Transformers for image recognition at scale. In: *Int. Conf. Learn. Represent.* (2020)
20. Fu, J., Liu, J., Tian, H., Li, Y., Bao, Y., Fang, Z., Lu, H.: Dual attention network for scene segmentation. In: *IEEE Conf. Comput. Vis. Pattern Recog.* pp. 3146–3154 (2019)
21. Gao, S.H., Cheng, M.M., Zhao, K., Zhang, X.Y., Yang, M.H., Torr, P.: Res2net: A new multi-scale backbone architecture. *IEEE Transactions on Pattern Analysis and Machine Intelligence* **43**(2), 652–662 (2021)
22. Geng, Z., Guo, M.H., Chen, H., Li, X., Wei, K., Lin, Z.: Is attention better than matrix decomposition? In: *Int. Conf. Learn. Represent.* (2021)
23. Gottlieb, J.P., Kusunoki, M., Goldberg, M.E.: The representation of visual salience in monkey parietal cortex. *Nature* **391**(6666), 481–484 (1998)
24. Guo, M.H., Cai, J.X., Liu, Z.N., Mu, T.J., Martin, R.R., Hu, S.M.: Pct: Point cloud transformer. *Computational Visual Media* **7**(2), 187–199 (2021)
25. Guo, M.H., Liu, Z.N., Mu, T.J., Hu, S.M.: Beyond self-attention: External attention using two linear layers for visual tasks. *arXiv preprint arXiv:2105.02358* (2021)
26. Guo, M.H., Liu, Z.N., Mu, T.J., Liang, D., Martin, R.R., Hu, S.M.: Can attention enable mlps to catch up with cnns? *Computational Visual Media* **7**(3), 283–288 (2021)
27. Guo, M.H., Xu, T.X., Liu, J.J., Liu, Z.N., Jiang, P.T., Mu, T.J., Zhang, S.H., Martin, R.R., Cheng, M.M., Hu, S.M.: Attention mechanisms in computer vision: A survey. *arXiv preprint arXiv:2111.07624* (2021)
28. Han, K., Xiao, A., Wu, E., Guo, J., Xu, C., Wang, Y.: Transformer in transformer. *Adv. Neural Inform. Process. Syst.* **34** (2021)
29. He, K., Chen, X., Xie, S., Li, Y., Dollár, P., Girshick, R.: Masked autoencoders are scalable vision learners (2021)
30. He, K., Gkioxari, G., Dollar, P., Girshick, R.: Mask r-cnn. In: *Int. Conf. Comput. Vis.* (Oct 2017)
31. He, K., Zhang, X., Ren, S., Sun, J.: Deep residual learning for image recognition. In: *IEEE Conf. Comput. Vis. Pattern Recog.* pp. 770–778 (2016)
32. Hendrycks, D., Gimpel, K.: Gaussian error linear units (gelus) (2020)
33. Howard, A.G., Zhu, M., Chen, B., Kalenichenko, D., Wang, W., Weyand, T., Andreetto, M., Adam, H.: Mobilenets: Efficient convolutional neural networks for mobile vision applications. *arXiv preprint arXiv:1704.04861* (2017)
34. Hu, H., Gu, J., Zhang, Z., Dai, J., Wei, Y.: Relation networks for object detection. In: *IEEE Conf. Comput. Vis. Pattern Recog.* pp. 3588–3597 (2018)
35. Hu, J., Shen, L., Albanie, S., Sun, G., Vedaldi, A.: Gather-excite: Exploiting feature context in convolutional neural networks. *Adv. Neural Inform. Process. Syst.* **31** (2018)
36. Hu, J., Shen, L., Sun, G.: Squeeze-and-excitation networks. In: *IEEE Conf. Comput. Vis. Pattern Recog.* pp. 7132–7141 (2018)
37. Huang, G., Liu, Z., Van Der Maaten, L., Weinberger, K.Q.: Densely connected convolutional networks. In: *IEEE Conf. Comput. Vis. Pattern Recog.* pp. 4700–4708 (2017)
38. Ioffe, S., Szegedy, C.: Batch normalization: Accelerating deep network training by reducing internal covariate shift. In: *Int. Conf. Mach. Learn.* pp. 448–456. *PMLR* (2015)

39. Kingma, D.P., Ba, J.: Adam: A method for stochastic optimization (2017)
40. Kirillov, A., Girshick, R., He, K., Dollár, P.: Panoptic feature pyramid networks. In: IEEE Conf. Comput. Vis. Pattern Recog. pp. 6399–6408 (2019)
41. Krizhevsky, A., Sutskever, I., Hinton, G.E.: Imagenet classification with deep convolutional neural networks. *Adv. Neural Inform. Process. Syst.* **25**, 1097–1105 (2012)
42. LeCun, Y., Boser, B., Denker, J.S., Henderson, D., Howard, R.E., Hubbard, W., Jackel, L.D.: Backpropagation applied to handwritten zip code recognition. *Neural computation* **1**(4), 541–551 (1989)
43. LeCun, Y., Bottou, L., Bengio, Y., Haffner, P.: Gradient-based learning applied to document recognition. *Proceedings of the IEEE* **86**(11), 2278–2324 (1998)
44. Li, X., Wang, W., Wu, L., Chen, S., Hu, X., Li, J., Tang, J., Yang, J.: Generalized focal loss: Learning qualified and distributed bounding boxes for dense object detection. *Adv. Neural Inform. Process. Syst.* **33**, 21002–21012 (2020)
45. Lin, M., Chen, Q., Yan, S.: Network in network. In: *Int. Conf. Learn. Represent.* (2014)
46. Lin, T.Y., Goyal, P., Girshick, R., He, K., Dollár, P.: Focal loss for dense object detection. In: *Int. Conf. Comput. Vis.* pp. 2980–2988 (2017)
47. Lin, T.Y., Maire, M., Belongie, S., Hays, J., Perona, P., Ramanan, D., Dollár, P., Zitnick, C.L.: Microsoft coco: Common objects in context. In: *Eur. Conf. Comput. Vis.* pp. 740–755. Springer (2014)
48. Liu, H., Dai, Z., So, D., Le, Q.V.: Pay attention to MLPs. In: Beygelzimer, A., Dauphin, Y., Liang, P., Vaughan, J.W. (eds.) *Adv. Neural Inform. Process. Syst.* (2021)
49. Liu, R., Deng, H., Huang, Y., Shi, X., Lu, L., Sun, W., Wang, X., Dai, J., Li, H.: Decoupled spatial-temporal transformer for video inpainting. *arXiv preprint arXiv:2104.06637* (2021)
50. Liu, R., Deng, H., Huang, Y., Shi, X., Lu, L., Sun, W., Wang, X., Dai, J., Li, H.: Fuseformer: Fusing fine-grained information in transformers for video inpainting. In: *Int. Conf. Comput. Vis.* pp. 14040–14049 (2021)
51. Liu, R., Li, Y., Tao, L., Liang, D., Hu, S.M., Zheng, H.T.: Are we ready for a new paradigm shift? a survey on visual deep mlp (2021)
52. Liu, S., Li, F., Zhang, H., Yang, X., Qi, X., Su, H., Zhu, J., Zhang, L.: DAB-DETR: Dynamic anchor boxes are better queries for DETR. In: *Int. Conf. Learn. Represent.* (2022)
53. Liu, S., Zhang, L., Yang, X., Su, H., Zhu, J.: Query2label: A simple transformer way to multi-label classification (2021)
54. Liu, Z., Lin, Y., Cao, Y., Hu, H., Wei, Y., Zhang, Z., Lin, S., Guo, B.: Swin transformer: Hierarchical vision transformer using shifted windows. In: *Int. Conf. Comput. Vis.* (2021)
55. Liu, Z., Mao, H., Wu, C.Y., Feichtenhofer, C., Darrell, T., Xie, S.: A convnet for the 2020s (2022)
56. Loshchilov, I., Hutter, F.: Sgdr: Stochastic gradient descent with warm restarts. *arXiv preprint arXiv:1608.03983* (2016)
57. Loshchilov, I., Hutter, F.: Decoupled weight decay regularization (2019)
58. Mnih, V., Heess, N., Graves, A., et al.: Recurrent models of visual attention. In: *Adv. Neural Inform. Process. Syst.* pp. 2204–2212 (2014)
59. Müller, R., Kornblith, S., Hinton, G.E.: When does label smoothing help? *Adv. Neural Inform. Process. Syst.* **32** (2019)
60. Park, J., Woo, S., Lee, J.Y., Kweon, I.S.: Bam: Bottleneck attention module. *arXiv preprint arXiv:1807.06514* (2018)

61. Polyak, B.T., Juditsky, A.B.: Acceleration of stochastic approximation by averaging. *SIAM journal on control and optimization* **30**(4), 838–855 (1992)
62. Qin, Z., Zhang, P., Wu, F., Li, X.: Fcanet: Frequency channel attention networks. In: *Int. Conf. Comput. Vis.* pp. 783–792 (2021)
63. Radosavovic, I., Kosaraju, R.P., Girshick, R., He, K., Dollár, P.: Designing network design spaces. In: *IEEE Conf. Comput. Vis. Pattern Recog.* pp. 10428–10436 (2020)
64. Ramachandran, P., Parmar, N., Vaswani, A., Bello, I., Levskaya, A., Shlens, J.: Stand-alone self-attention in vision models. *arXiv preprint arXiv:1906.05909* (2019)
65. Rosenblatt, F.: The perceptron: a probabilistic model for information storage and organization in the brain. *Psychological review* **65**(6), 386 (1958)
66. Rumelhart, D.E., Hinton, G.E., Williams, R.J.: Learning internal representations by error propagation. Tech. rep., California Univ San Diego La Jolla Inst for Cognitive Science (1985)
67. Sandler, M., Howard, A., Zhu, M., Zhmoginov, A., Chen, L.C.: Mobilenetv2: Inverted residuals and linear bottlenecks. In: *IEEE Conf. Comput. Vis. Pattern Recog.* pp. 4510–4520 (2018)
68. Selvaraju, R.R., Cogswell, M., Das, A., Vedantam, R., Parikh, D., Batra, D.: Grad-cam: Visual explanations from deep networks via gradient-based localization. In: *Int. Conf. Comput. Vis.* pp. 618–626 (2017)
69. Sermanet, P., Eigen, D., Zhang, X., Mathieu, M., Fergus, R., LeCun, Y.: Overfeat: Integrated recognition, localization and detection using convolutional networks. *arXiv preprint arXiv:1312.6229* (2013)
70. Simonyan, K., Zisserman, A.: Very deep convolutional networks for large-scale image recognition. *arXiv preprint arXiv:1409.1556* (2014)
71. Srinivas, A., Lin, T.Y., Parmar, N., Shlens, J., Abbeel, P., Vaswani, A.: Bottleneck transformers for visual recognition. In: *IEEE Conf. Comput. Vis. Pattern Recog.* pp. 16519–16529 (2021)
72. Sun, P., Zhang, R., Jiang, Y., Kong, T., Xu, C., Zhan, W., Tomizuka, M., Li, L., Yuan, Z., Wang, C., et al.: Sparse r-cnn: End-to-end object detection with learnable proposals. In: *IEEE Conf. Comput. Vis. Pattern Recog.* pp. 14454–14463 (2021)
73. Szegedy, C., Liu, W., Jia, Y., Sermanet, P., Reed, S., Anguelov, D., Erhan, D., Vanhoucke, V., Rabinovich, A.: Going deeper with convolutions. In: *IEEE Conf. Comput. Vis. Pattern Recog.* pp. 1–9 (2015)
74. Tolstikhin, I.O., Houlsby, N., Kolesnikov, A., Beyer, L., Zhai, X., Unterthiner, T., Yung, J., Steiner, A., Keysers, D., Uszkoreit, J., et al.: Mlp-mixer: An all-mlp architecture for vision. *Adv. Neural Inform. Process. Syst.* **34** (2021)
75. Touvron, H., Bojanowski, P., Caron, M., Cord, M., El-Nouby, A., Grave, E., Izacard, G., Joulin, A., Synnaeve, G., Verbeek, J., et al.: Resmlp: Feedforward networks for image classification with data-efficient training. *arXiv preprint arXiv:2105.03404* (2021)
76. Touvron, H., Cord, M., Douze, M., Massa, F., Sablayrolles, A., Jégou, H.: Training data-efficient image transformers & distillation through attention. In: *Int. Conf. Mach. Learn.* pp. 10347–10357. PMLR (2021)
77. Touvron, H., Cord, M., Sablayrolles, A., Synnaeve, G., Jégou, H.: Going deeper with image transformers. In: *Int. Conf. Comput. Vis.* pp. 32–42 (2021)
78. Treisman, A.M., Gelade, G.: A feature-integration theory of attention. *Cognitive psychology* **12**(1), 97–136 (1980)

79. Tsotsos, J.K., Culhane, S.M., Wai, W.Y.K., Lai, Y., Davis, N., Nuflo, F.: Modeling visual attention via selective tuning. *Artificial intelligence* **78**(1-2), 507–545 (1995)
80. Vaswani, A., Shazeer, N., Parmar, N., Uszkoreit, J., Jones, L., Gomez, A.N., Kaiser, L., Polosukhin, I.: Attention is all you need. In: *Adv. Neural Inform. Process. Syst.* pp. 5998–6008 (2017)
81. Wang, F., Jiang, M., Qian, C., Yang, S., Li, C., Zhang, H., Wang, X., Tang, X.: Residual attention network for image classification. In: *IEEE Conf. Comput. Vis. Pattern Recog.* pp. 3156–3164 (2017)
82. Wang, J., Sun, K., Cheng, T., Jiang, B., Deng, C., Zhao, Y., Liu, D., Mu, Y., Tan, M., Wang, X., et al.: Deep high-resolution representation learning for visual recognition. *IEEE transactions on pattern analysis and machine intelligence* (2020)
83. Wang, Q., Wu, B., Zhu, P., Li, P., Zuo, W., Hu, Q.: Eca-net: Efficient channel attention for deep convolutional neural networks (2020)
84. Wang, W., Xie, E., Li, X., Fan, D.P., Song, K., Liang, D., Lu, T., Luo, P., Shao, L.: Pvtv2: Improved baselines with pyramid vision transformer. *arXiv preprint arXiv:2106.13797* (2021)
85. Wang, W., Xie, E., Li, X., Fan, D.P., Song, K., Liang, D., Lu, T., Luo, P., Shao, L.: Pyramid vision transformer: A versatile backbone for dense prediction without convolutions. In: *Int. Conf. Comput. Vis.* (2021)
86. Wang, X., Girshick, R., Gupta, A., He, K.: Non-local neural networks. In: *IEEE Conf. Comput. Vis. Pattern Recog.* pp. 7794–7803 (2018)
87. Wolfe, J.M., Horowitz, T.S.: What attributes guide the deployment of visual attention and how do they do it? *Nature reviews neuroscience* **5**(6), 495–501 (2004)
88. Woo, S., Park, J., Lee, J.Y., Kweon, I.S.: Cbam: Convolutional block attention module. In: *Eur. Conf. Comput. Vis.* pp. 3–19 (2018)
89. Wu, H., Xiao, B., Codella, N., Liu, M., Dai, X., Yuan, L., Zhang, L.: Cvt: Introducing convolutions to vision transformers. In: *Int. Conf. Comput. Vis.* pp. 22–31 (2021)
90. Xiao, T., Liu, Y., Zhou, B., Jiang, Y., Sun, J.: Unified perceptual parsing for scene understanding. In: *Eur. Conf. Comput. Vis.* pp. 418–434 (2018)
91. Xie, E., Wang, W., Yu, Z., Anandkumar, A., Alvarez, J.M., Luo, P.: Segformer: Simple and efficient design for semantic segmentation with transformers. *Adv. Neural Inform. Process. Syst.* **34** (2021)
92. Xie, S., Girshick, R., Dollár, P., Tu, Z., He, K.: Aggregated residual transformations for deep neural networks. In: *IEEE Conf. Comput. Vis. Pattern Recog.* pp. 1492–1500 (2017)
93. Xie, S., Liu, S., Chen, Z., Tu, Z.: Attentional shapecontextnet for point cloud recognition. In: *IEEE Conf. Comput. Vis. Pattern Recog.* pp. 4606–4615 (2018)
94. Yang, J., Li, C., Zhang, P., Dai, X., Xiao, B., Yuan, L., Gao, J.: Focal self-attention for local-global interactions in vision transformers (2021)
95. Yu, F., Koltun, V.: Multi-scale context aggregation by dilated convolutions. *arXiv preprint arXiv:1511.07122* (2015)
96. Yu, W., Luo, M., Zhou, P., Si, C., Zhou, Y., Wang, X., Feng, J., Yan, S.: Metaformer is actually what you need for vision. *arXiv preprint arXiv:2111.11418* (2021)
97. Yuan, L., Chen, Y., Wang, T., Yu, W., Shi, Y., Jiang, Z.H., Tay, F.E., Feng, J., Yan, S.: Tokens-to-token vit: Training vision transformers from scratch on imagenet. In: *Int. Conf. Comput. Vis.* pp. 558–567 (October 2021)

98. Yuan, Y., Chen, X., Wang, J.: Object-contextual representations for semantic segmentation. In: *Computer Vision–ECCV 2020: 16th European Conference, Glasgow, UK, August 23–28, 2020, Proceedings, Part VI* 16. pp. 173–190. Springer (2020)
99. Yuan, Y., Huang, L., Guo, J., Zhang, C., Chen, X., Wang, J.: Ocnet: Object context network for scene parsing. *arXiv preprint arXiv:1809.00916* (2018)
100. Yun, S., Han, D., Oh, S.J., Chun, S., Choe, J., Yoo, Y.: Cutmix: Regularization strategy to train strong classifiers with localizable features. In: *Int. Conf. Comput. Vis.* pp. 6023–6032 (2019)
101. Zhang, H., Goodfellow, I., Metaxas, D., Odena, A.: Self-attention generative adversarial networks. In: *Int. Conf. Mach. Learn.* pp. 7354–7363. PMLR (2019)
102. Zhang, H., Cisse, M., Dauphin, Y.N., Lopez-Paz, D.: mixup: Beyond empirical risk minimization. *arXiv preprint arXiv:1710.09412* (2017)
103. Zhang, S., Chi, C., Yao, Y., Lei, Z., Li, S.Z.: Bridging the gap between anchor-based and anchor-free detection via adaptive training sample selection. In: *IEEE Conf. Comput. Vis. Pattern Recog.* pp. 9759–9768 (2020)
104. Zhang, X., Zhou, X., Lin, M., Sun, J.: Shufflenet: An extremely efficient convolutional neural network for mobile devices. In: *IEEE Conf. Comput. Vis. Pattern Recog.* pp. 6848–6856 (2018)
105. Zhong, Z., Zheng, L., Kang, G., Li, S., Yang, Y.: Random erasing data augmentation. In: *AAAI Conf. Artif. Intell.* pp. 13001–13008 (2020)
106. Zhou, B., Khosla, A., Lapedriza, A., Oliva, A., Torralba, A.: Learning deep features for discriminative localization. In: *IEEE Conf. Comput. Vis. Pattern Recog.* pp. 2921–2929 (2016)
107. Zhou, B., Zhao, H., Puig, X., Xiao, T., Fidler, S., Barriuso, A., Torralba, A.: Semantic understanding of scenes through the ade20k dataset. *Int. J. Comput. Vis.* **127**(3), 302–321 (2019)